

Artificial neural networks for sheet sediment transport

GOKMEN TAYFUR

*Department of Civil Engineering, Izmir Institute of Technology, Urla 35347, Izmir, Turkey
tayfur@likya.iyte.edu.tr*

Abstract Sheet sediment transport was modelled by artificial neural networks (ANNs). A three-layer feed-forward artificial neural network structure was constructed and a back-propagation algorithm was used for the training of ANNs. Event-based, runoff-driven experimental sediment data were used for the training and testing of the ANNs. In training, data on slope and rainfall intensity were fed into the network as inputs and data on sediment discharge were used as target outputs. The performance of the ANNs was tested against that of the most commonly used physically-based models, whose transport capacity was based on one of the dominant variables—flow velocity (V), shear stress (SS), stream power (SP), and unit stream power (USP). The comparison results revealed that the ANNs performed as well as the physically-based models for simulating nonsteady-state sediment loads from different slopes. The performances of the ANNs and the physically-based models were also quantitatively investigated to estimate mean sediment discharges from experimental runs. The investigation results indicated that better estimations were obtained for V over mild and steep slopes, under low rainfall intensity; for USP over mild and steep slopes, under high rainfall intensity; for SP and SS over very steep slopes, under high rainfall intensity; and for ANNs over steep and very steep slopes, under very high rainfall intensities.

Key words sediment transport; artificial neural networks; transport capacity

Application des réseaux de neurones artificiels pour le transport sédimentaire en nappe

Résumé Le transport sédimentaire en nappe a été modélisé par des réseaux de neurones artificiels. Une structure de réseau de neurones artificiel à trois couches et progressif a été construite, et un algorithme de rétro-propagation a été utilisé pour l'apprentissage. Des données expérimentales événementielles de transport de sédiment par ruissellement ont été utilisées pour l'apprentissage et le test des réseaux de neurones artificiels. Lors de l'apprentissage, des données de pente et d'intensité de précipitation ont été fournies au réseau en guise de données d'entrée et des données de débit solide ont servi de cible pour les sorties. La performance des réseaux de neurones artificiels a été testée par comparaison avec celles des modèles à bases physiques les plus communs, dont la capacité de transport est basée sur l'une des variables dominantes—vitesse d'écoulement, contrainte tangentielle, puissance du cours d'eau et puissance unitaire du cours d'eau. La comparaison des résultats a révélé que les réseaux de neurones ont des performances semblables à celles des modèles à bases physiques pour simuler les charges sédimentaires en état non-stationnaire, pour diverses pentes. Cette comparaison des performances a également été menée de manière quantitative pour l'estimation des débits solides moyens expérimentaux. Les meilleures simulations ont été obtenues sur la base de la vitesse d'écoulement pour des pentes douces à fortes et pour de faibles intensités de précipitation; sur la base de la puissance unitaire du cours d'eau pour des pentes douces à fortes et pour de fortes intensités; sur la base de la puissance du cours d'eau et de la contrainte tangentielle pour de très fortes pentes et pour de fortes intensités; et avec les réseaux de neurones artificiels pour de fortes et très fortes pentes et pour de très fortes intensités.

Mots clefs transport solide; réseaux de neurones artificiels; capacité de transport

INTRODUCTION

Sheet sediment transport is mainly modelled by black-box models (Guldal & Muftuoglu 2001), regression-based models (Leaf 1974; Megahan 1974) and physically-based

models (Li 1979; Foster 1982; Govindaraju & Kavvas 1991). The physically-based models are improvements over the black-box, and regression-based models and they represent the physical laws. Most of the physically-based models have a continuity equation for sediment mass conservation and another equation that relates sediment load to the flow transport capacity.

Flow transport capacity is determined by a dominant variable such as flow discharge, velocity, slope, shear stress, unit stream power, and stream power. To simulate steady-state sediment loads, shear stress, unit stream power, and stream power approaches have found a wide application (Smith 1976; Alonso *et al.*, 1981; Foster 1982; Moore & Burch 1986; Rose *et al.*, 1983a,b). To simulate nonsteady-state loads, the shear stress approach has been commonly employed (Li 1979; Woolhiser *et al.*, 1990; Govindaraju & Kavvas, 1991; Tayfur, 2001). Tayfur (2002) investigated the applicability of shear stress, stream power, and unit stream power transport capacity models for simulating nonsteady-state loads from steep slopes.

No matter which flow transport capacity approach is used, a physically-based model typically involves a solution of a system of nonlinear partial differential equations. For most problems, a numerical solution is sought by discretizing time-space dimensions into a discrete set of nodes. This implies that such models work best when data on the physical characteristics of the domain are available at the model grid scale. However, these kind of data are rarely available, even in heavily instrumented watersheds. On the other hand, the utilization of spatially-varying data generally results in numerical convergence and instability problems (Tayfur *et al.*, 1993). It is perhaps because of such problems that researchers are still looking for alternative new modelling techniques.

One of the new modelling techniques is the artificial neural networks (ANNs) method. The method has an ability to identify a relationship from given patterns and this makes it possible for ANNs to solve large-scale complex problems such as pattern recognition, nonlinear modelling, classification, association, and control. This is the reason that, in this last decade, ANNs have been commonly employed to solve hydrology-related problems such as rainfall–runoff modelling, streamflow forecasting, groundwater modelling, water quality, water management policy, precipitation forecasting, hydrological time series, and reservoir operation.

Several studies attempted to model runoff by ANNs. For example, Halff *et al.* (1993) designed a three-layer feed-forward ANN using the observed rainfall hyetographs as inputs and hydrographs as outputs to predict runoff from a watershed at Bellevue, Washington, USA. Their study opened up several possibilities for rainfall–runoff applications using neural networks. Smith & Eli (1995) applied a back-propagation neural network model to predict peak discharge and time to peak over a hypothetical watershed. They were able to incorporate the spatial and temporal distribution of rainfall into the ANN model. Tokar & Johnson (1999) successfully forecast daily runoff for a river in Maryland, USA with daily precipitation, temperature, and snowmelt equivalent serving as inputs to the neural network. Many other studies involved forecasting of hourly, daily, and monthly streamflows and flow discharges by ANNs. For example, Kang *et al.* (1993) used ANNs and an autoregressive moving average model (ARMA) to predict hourly and daily streamflows in a river in Korea. They pointed out that the ANN model performed as well as the ARMA model. Marcus *et al.* (1995) used ANNs and periodic transfer functions (PTFs)

to predict monthly streamflows at a gauging station in Colorado, USA. They pointed out that both models were good at predicting streamflows. Tawfik *et al.* (1997) used ANNs with a saturating linear transfer function to predict flow discharges at two locations over the River Nile using the stage and the rate of change of stage as network inputs. They showed that ANNs satisfactorily predicted the discharges. The usefulness of ANNs was also illustrated for estimating aquifer parameter values (Aziz & Wong, 1992), salinity (Maier & Dandy, 1996; Huang & Foo, 2002), saturated hydraulic conductivity (Morshed & Kaluarachchi, 1998), water content (Persson *et al.*, 2001), missing data (Elshorbagy *et al.*, 2001), rainfall from remotely sensed images of clouds (Tohma & Igata, 1994) and from satellite infrared images (Hsu *et al.*, 1996), and changes in streamflow conditions due to the variations in climate (Cannon & Whitfield, 2002).

The objective of this study is to simulate sheet sediment transport by ANNs. The performance of the ANNs will be compared to that of physically-based models.

MATHEMATICAL BACKGROUND

Artificial neural networks (ANNs)

In applications, a three-layer feed-forward type of artificial neural network is generally considered (Fig. 1). In a feed-forward network, the input quantities are fed into input layer neurons, which, in turn, pass them on to the hidden-layer neurons after multiplying by a weight. A hidden-layer neuron adds up the weighted input received from each input neuron, associates it with a bias, and then passes the result on through a nonlinear transfer function. The output neurons perform the same operation as that of a hidden neuron.

Before its application to any problem, the network is first trained, whereby the target output at each output neuron is minimized by adjusting the weights and biases

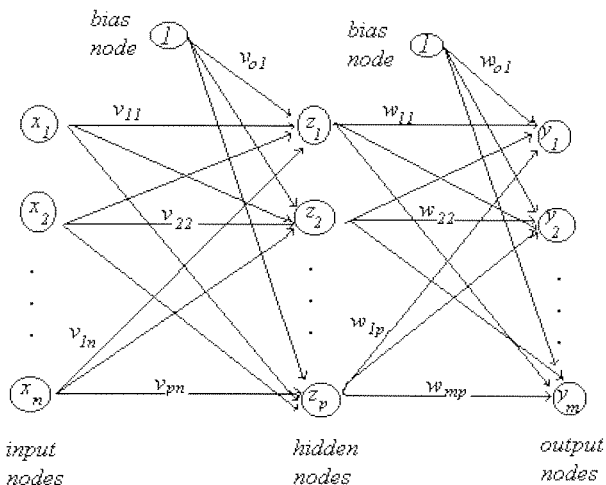


Fig. 1 Schematic representation of a feed-forward three-layer ANN.

through some training algorithm. Training in ANNs consists of three elements: (a) weights between neurons that define the relative importance of the inputs; (b) a transfer function that controls the generation of the output from a neuron; and (c) a set of learning laws that describe how the adjustments of the weights are made during training.

During training, a neuron receives inputs from previous layers, weights each input with a prearranged value, and combines these weighted inputs (Fig. 2). The combination of the weighted inputs is represented as:

$$net_j = \sum x_i v_{ij} - b_j \quad (1)$$

where net_j is the summation of the weighted input for the j th neuron; x_i is the input from the i th neuron to the j th neuron; v_{ij} is the weight from the i th neuron in the previous layer to the j th neuron in the current layer; and b_j is the threshold value, also called the bias, associated with node j (Fig. 2). In ANNs, the bias of the node must be exceeded before it can be activated.

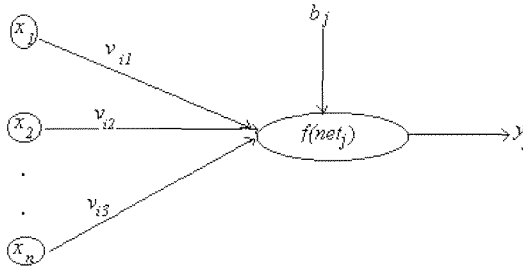


Fig. 2 Schematic diagram of a hidden-layer neuron.

The net_j value is passed through a transfer function to determine the level of activation. If the activation of a neuron is strong enough, it produces an output that is sent as an input to other neurons in the successive layer. Generally, the sigmoid function is employed as an activation function in the training of the network. The sigmoid function is expressed as:

$$f(net_j) = \frac{1}{1 + e^{-net_j}} \quad (2)$$

The learning of ANNs is generally accomplished by a back-propagation algorithm. The back-propagation is the most commonly used supervised training algorithm in the multilayered feed-forward networks. In back-propagation networks, information is processed in the forward direction from the input layer to the hidden layer and then to the output layer (Fig. 1). The objective of a back-propagation network is, by minimizing a predetermined error function, to find the optimal weights which would generate an output vector $\mathbf{Y} = (y_1, y_2, \dots, y_p)$ as close as possible to target values of output vector $\mathbf{T} = (t_1, t_2, \dots, t_p)$ with a selected accuracy.

A predetermined error function has the following form (ASCE, 2000):

$$E = \sum_P \sum_p (y_i - t_i)^2 \quad (3)$$

where y_i is the component of an ANN output vector \mathbf{Y} ; t_i is the component of a target output vector \mathbf{T} ; p is the number of output neurons; and P is the number of training patterns.

The least square error method, along with a generalized delta rule, is used to optimize the network weights. The gradient descent method, along with the chain rule of derivatives, is employed to modify network weights as:

$$v_{ij}^{\text{new}} = v_{ij}^{\text{old}} - \delta \frac{\partial E}{\partial v_{ij}} \quad (4)$$

where δ is the learning rate which is used to increase the chance of avoiding the training process being trapped in a local minimum instead of a global minimum.

The details of ANNs can be obtained from Dawson & Wilby (1998), Tokar & Johnson (1999), and ASCE (2000a,b).

Physically-based model

Sheet sediment transport based on kinematic wave approximation, in one dimension, is mathematically expressed by a pair of following nonlinear partial differential equations (Tayfur, 2002):

$$\frac{\partial h}{\partial t} + \frac{\partial}{\partial x} \left(\frac{\sqrt{S}}{n} h^{5/3} \right) = (r - i) \quad (5)$$

$$\frac{\partial(hc)}{\partial t} + \frac{\partial}{\partial x} \left(\frac{\sqrt{S}}{n} h^{5/3} c \right) = \frac{1}{\rho_s} (D_{rd} + D_{fd}) \quad (6)$$

where h is the flow depth; r is the rainfall intensity; i is the infiltration rate; S is the bed-slope; n is the Manning's roughness coefficient; c is the sediment concentration by volume; ρ_s is the sediment particle density; D_{rd} is the soil detachment rate by raindrops; and D_{fd} is the soil detachment/deposition rate by sheet flow.

On a bare soil surface, soil detachment by raindrops can be expressed as (Li, 1979):

$$D_{rd} = \alpha r^\beta \left(1 - \frac{z_w}{6.69r^{0.182}} \right) \quad (7)$$

where α is the soil detachability coefficient whose range is 0.0006–0.0086 kg m⁻² mm⁻¹ (Sharma *et al.*, 1993); β is an exponent whose range is 1.0–2.0; and z_w is the flow depth plus the loose soil depth.

The soil detachment and deposition by sheet flow can be expressed as (Foster, 1982):

$$D_{fd} = \varphi(T_c - q_s) \quad (8)$$

where q_s is the unit sediment discharge:

$$q_s = \rho_s c \frac{\sqrt{S}}{n} h^{5/3} \quad (9)$$

and T_c is the sediment transport capacity. If the transport capacity exceeds the existing unit sediment discharge ($T_c > q_s$), the flow will detach particles, otherwise it will deposit the particles. The term ϕ is the transfer rate coefficient whose range is 3–33 m^{-1} (Foster, 1982).

The transport capacity is expressed by the following basic form (Yang, 1996):

$$T_c = \eta_i (D - D_c)^{k_i} \quad (10)$$

where η_i is the soil erodibility coefficient whose range is 0.0–1.0 and k_i is an exponent whose value varies between 1 and 2.5 (Foster, 1982). The parameter D is a dominant variable and D_c is the critical condition of the dominant variable at incipient motion.

In a physically-based model, the transport capacity would be expressed as a function of different dominant variables. Depending upon the choice of the dominant variable, one may end up with different transport capacity models. In this study, the dominant variable (D) was chosen to be flow velocity (V), shear stress (τ), stream power (τV), and unit stream power ($V S$). Similarly, the critical dominant variable (D_c) was chosen to be critical flow velocity (V_c), critical shear stress (τ_c), critical stream power ($\tau_c V_c$), and critical unit stream power ($V_c S_c$). Hence, velocity, shear stress, stream power, and unit stream power approaches were employed in this study.

Flow velocity (V) is computed from equation (5) and is equal to $\frac{\sqrt{S}}{n} h^{2/3}$. The critical flow velocity is expressed as function of fall velocity and the shear velocity Reynolds number and given in Yang (1996). Shear stress (τ) is equal to $\gamma h S$, where γ is the specific weight of water. Critical shear stress (τ_c) is expressed as a function of particle diameter and the specific weights of water and sediment and given in Li (1979). The critical slope is expressed as a function of roughness coefficient, flow depth, and particle diameters of d_{50} and d_{90} , and given in Yang (1996). The details of the transport capacity models are given in Tayfur (2002).

Equations (5) and (6) are solved simultaneously for each time step. From the solution of equation (5), flow depths and unit flow discharges are computed. The computed flow variables are then used in the solution of equation (6) to calculate sediment concentrations and unit sediment discharges. The details of the modelling are given in Tayfur (2002).

APPLICATION

The ANNs and the physically-based models were applied to simulate experimentally observed nonsteady-state sediment discharge data. For this purpose, the experimental data of Kilinc & Richardson (1973) were employed. Kilinc & Richardson (1973) performed experimental studies using a 1.52 m wide by 4.58 m long flume with an adjustable slope. The flume was filled with compacted sandy soil. The soil had a nonuniform size distribution with d_{50} of 0.35 mm, d_{90} of 1.3 mm, bulk density of

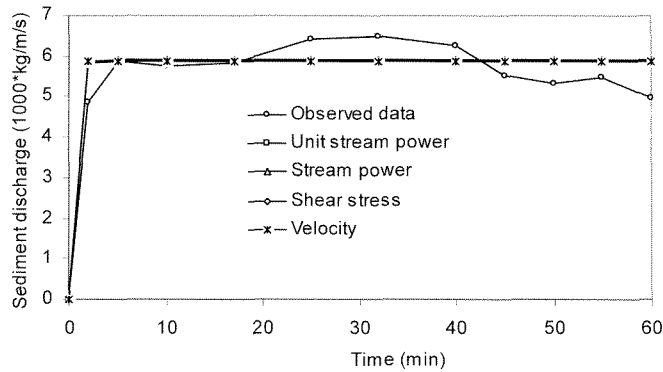


Fig. 3 Simulation of observed data: calibration run ($S = 20\%$; $r = 57$ mm).

1500 kg m^{-3} and porosity of 0.43. Six bare slopes of 5.7, 10, 15, 20, 30 and 40% were tested with four different rainfall intensities of 32, 57, 93 and 117 mm h^{-1} . On average, the constant infiltration rate for each run was about 5.3 mm h^{-1} .

One of the data sets of Kilinc & Richardson (1973) was used for the calibration of the parameters of the physically-based model. Figure 3 shows the calibration run for the case of 57 mm h^{-1} rainfall intensity over a 20% slope. The calibrated values of the model parameters are $n = 0.012$; $\alpha = 0.0012$; $\beta = 1.0$; $\eta_i = 0.10$; and $k_i = 1.56, 1.18, 1.92,$ and 2.36 for the unit stream power, stream power, shear stress, and velocity approaches, respectively. These values are within the ranges suggested in the literature (Woolhiser, 1974; Li, 1979; Foster, 1982; Sharma *et al.*, 1993).

In this study, a three-layer feed-forward artificial neural network structure was constructed. The model had two neurons in the input layer, eight neurons in the hidden layer, and one neuron in the output layer. For the number of neurons in the hidden layer, the trial-and-error procedure was used. The sigmoid function was employed as an activation function in the training of the network and the learning of the ANNs was accomplished by the back-propagation algorithm. Before starting the training process, a random value of 0.2, and -1.0 were assigned for the network weights and biases, respectively. These assigned values were consistent with the literature (Dawson & Wilby, 1998; ASCE, 2000). Also, due to the nature of the sigmoid function used in the back-propagation algorithm, it was prudent to standardize (i.e. convert to the range (0,1)) all external input and output values before passing them into a neural network. Without standardization, large values input into an ANN would require extremely small weighting factors to be applied and this can cause a number of problems (Dawson & Wilby, 1998). There are no fixed rules as to which standardization approach should be used in particular circumstances (Dawson & Wilby, 1998). In this study, the following standardization approach was employed:

$$z_i = \frac{x_i}{x_{\max} + 1} \quad (11)$$

where z_i is the standardized value; x_i is the input value; x_{\max} is the maximum input value.

The training of ANNs was accomplished by employing the experimental data from 18 runs. These included experiments over 5.7, 10, 15, 20, 30, and 40% slopes under

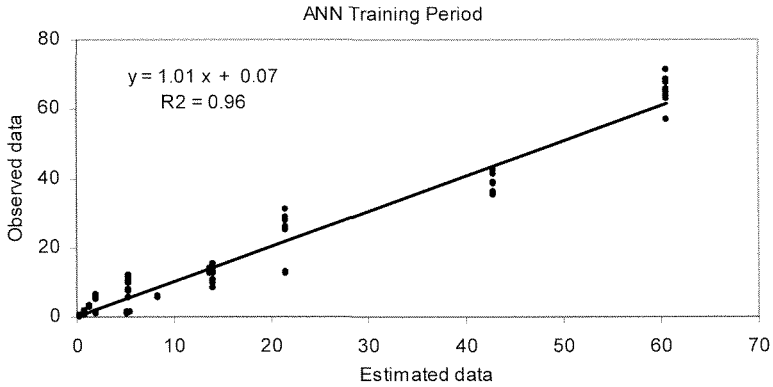


Fig. 4 Performance of ANN model—training.

32, 57, and 117 mm h⁻¹ rainfall intensities. The total number of observed sediment discharge data from these experiments was 164. Data on slope and rainfall intensities were fed into the system as input variables and the observed sediment discharge data were target output variables. The training of the model was accomplished with 0.01 learning rate and after 6000 iterations. Figure 4 shows the observed data vs corresponding ANNs output data at the end of the training. As can be seen from Fig. 4, the correlation coefficient (R^2) is 0.96 and the slope of the related regression curve is almost one and the y -intercept is almost zero. This implies that the training of the ANN model was accomplished.

The trained ANNs and calibrated physically-based models were applied to simulate observed sediment discharges from six runs which involved experiments over 5.7, 10, 15, 20, 30, and 40% slopes under 93 mm h⁻¹ rainfall intensity.

Figures 5–10 show the model simulations of the observed data over 5.7, 10, 15, 20, 30, and 40% slopes, respectively. The unit stream power (USP) model simulated the observed data from 5.7% quite well (Fig. 5). However, it underestimated the sediment loads from steep slopes of 10, 15 and 20% (Figs 6, 7 and 8). The performance of USP was good in estimating sediment discharges from very steep slopes of 30 and 40%

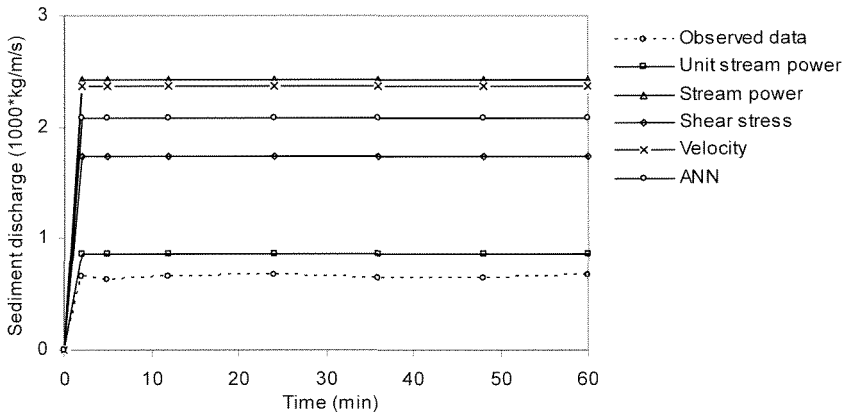


Fig. 5 Simulation of observed data ($S = 5.7\%$; $r = 93 \text{ mm h}^{-1}$).

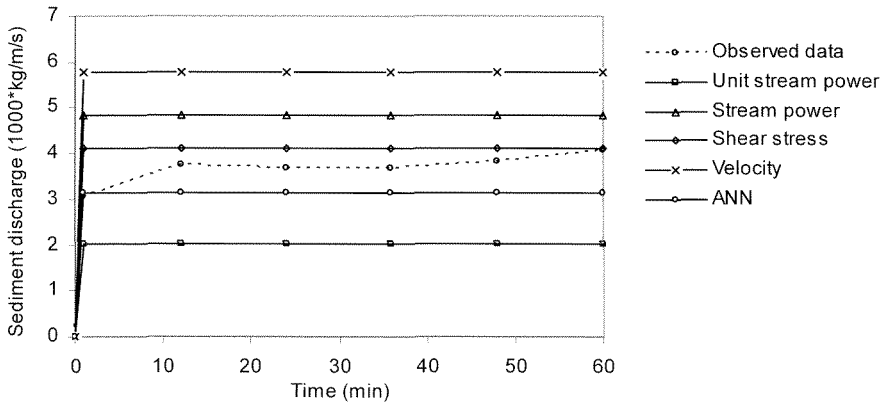


Fig. 6 Simulation of observed data ($S = 10\%$; $r = 93 \text{ mm h}^{-1}$).

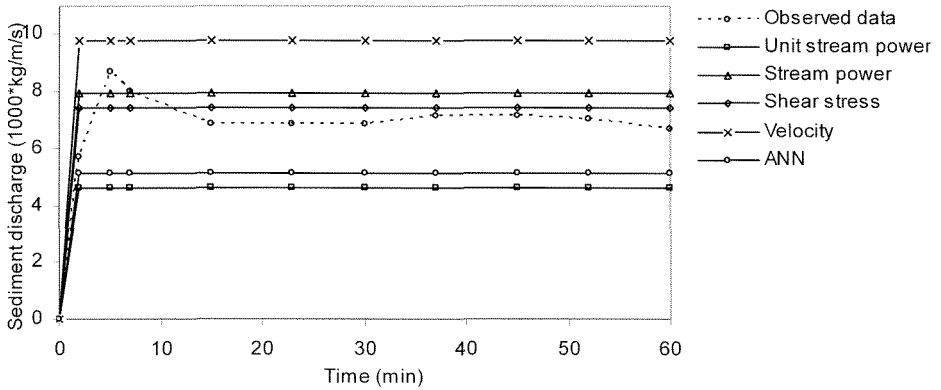


Fig. 7 Simulation of observed data ($S = 15\%$; $r = 93 \text{ mm h}^{-1}$).

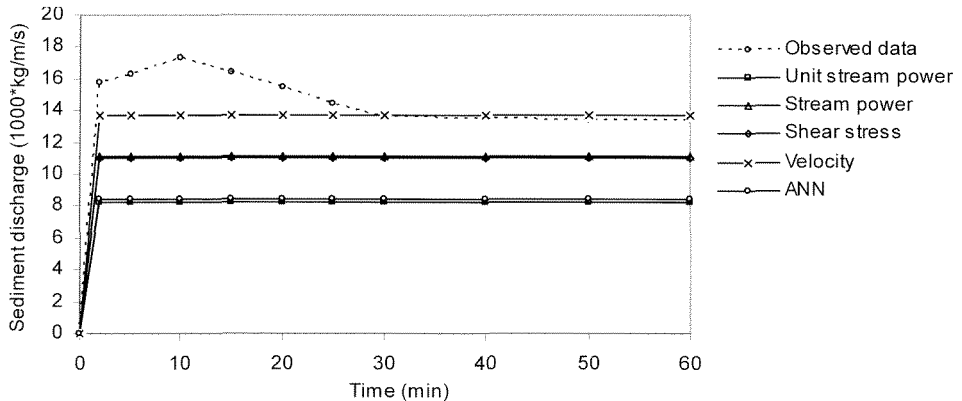


Fig. 8 Simulation of observed data ($S = 20\%$; $r = 93 \text{ mm h}^{-1}$).

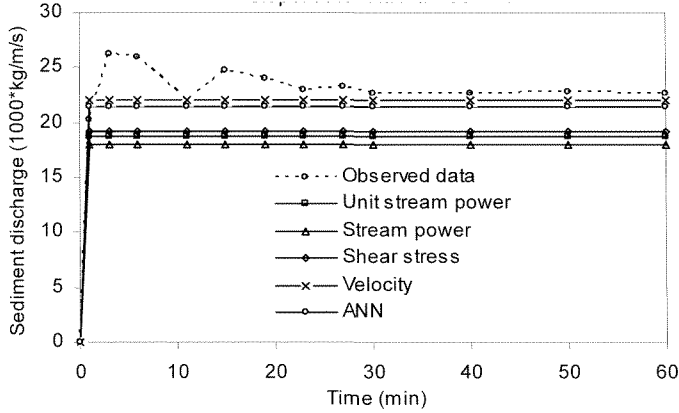


Fig. 9 Simulation of observed data ($S = 30\%$; $r = 93 \text{ mm h}^{-1}$).

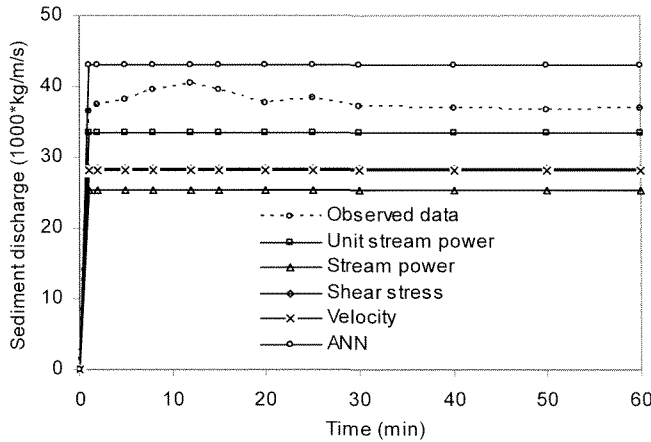


Fig. 10 Simulation of observed data ($S = 40\%$; $r = 93 \text{ mm h}^{-1}$).

(Figs 9 and 10). The stream power (SP) and the shear stress (SS) models simulated the sediment loads from steep slopes of 10, 15, and 20% satisfactorily (Figs 6, 7 and 8). However, they overestimated the loads from the 5.7% slope (Fig. 5) and underestimated the loads from very steep slopes of 30, and 40% (Figs 9 and 10). The velocity approach (V) gave very good simulations of very steep slopes of 20 and 30% (Figs 8 and 9). It overestimated loads from 5.7, 10 and 15% slopes (Figs 5, 6 and 7) and underestimated loads from the 40% slope (Fig. 10). The ANN model simulated loads from 10, 15, 30, and 40% slopes quite satisfactorily (Figs 6, 7, 9 and 10). Like most of the physically-based models, it overestimated loads from the 5.7% slope (Fig. 5) and underestimated loads from the 20% slope (Fig. 8).

The performances of the ANN model and the physically-based models were also investigated in terms of estimating observed mean sediment discharges of the 24 experimental runs. For this purpose, the ANN model was retrained. The total number of observed sediment discharge data from the 24 runs was 221. The slope and rainfall

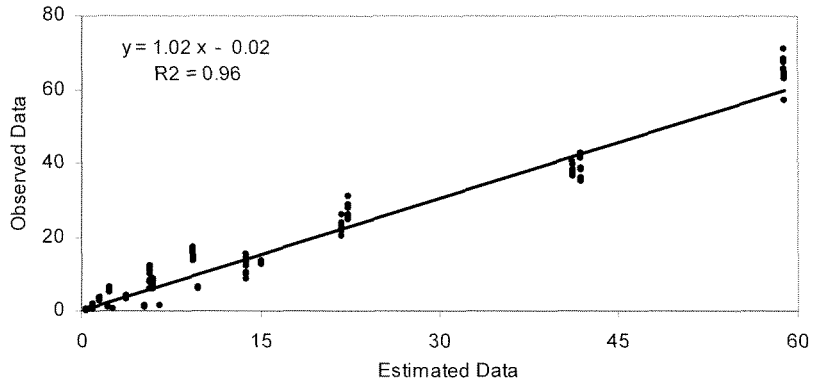


Fig. 11 Performance of ANN model—after retraining.

intensity data were fed into the system as inputs and the sediment discharge data were the target outputs. Figure 11 shows the observed sediment discharge data vs the estimated data by ANNs at the end of the training period. As can be seen in Fig. 11,

Table 1 The ANN model vs physically-based models for mean loads ($1000 \text{ kg m}^{-1} \text{ s}^{-1}$).

	5.7%	10%	15%	20%	30%	40%
32 mm h⁻¹:						
Observed	0.10	0.29	0.56	0.63	0.93	1.35
USP	0.33	0.96	2.19	3.92	8.87	15.86
SP	0.49	1.07	1.84	2.62	4.32	6.11
SS	0.36	0.95	1.77	2.68	4.72	7.03
V	0.06*	0.23*	0.82	1.56	3.19	4.89
ANNs	0.35	0.46	0.66*	0.96*	2.18*	5.27
57 mm h⁻¹:						
Observed	0.30	1.50	2.81	5.71	10.17	13.08
USP	0.52*	1.44*	3.27*	5.86 [†]	13.32	23.86
SP	1.28	2.58	4.20	5.91 [†]	9.54*	13.40*
SS	0.84	2.12	3.92	5.87 [†]	10.29*	15.19*
V	0.50*	1.97	3.89	5.89 [†]	9.83*	13.68*
ANNs	0.74	1.02	1.53	2.33	5.67	13.85*
93 mm h⁻¹:						
Observed	0.65	3.68	7.11	14.95	23.10	37.96
USP	0.86*	2.02	4.60	8.23	18.70	33.51
SP	2.43	4.85	7.92*	11.16	18.02	25.30
SS	1.73	4.13	7.41*	11.07	19.21	28.33
V	2.37	5.78	9.78	13.68*	22.07*	28.16
ANNs	2.60	3.80*	5.96*	9.37	21.80*	41.22*
117 mm h⁻¹:						
Observed	1.48	5.97	12.89	26.55	37.53	65.11
USP	0.85*	2.36	5.35	9.59	21.79	38.99
SP	3.17	6.43*	10.53*	14.87	24.03	33.74
SS	2.30	5.42*	9.88*	14.65	25.47	37.56
V	3.95	8.69	14.07*	19.25	28.96	38.19
ANNs	6.57	9.68	14.98*	22.42*	41.96*	58.85*

* Good estimations of the related observed data.

[†] Calibration run for the physically-based models.

the correlation coefficient (R^2) for this case is 0.96, the slope of the related regression equation is almost one and the y -intercept of the equation is very close to zero. These results indicate that the re-training of the ANNs was successfully accomplished.

The re-trained ANNs and the physically-based models were applied to estimate mean sediment discharges of the 24 runs. Table 1 presents the observed and model-estimated mean sediment discharges. In order to summarize the results further, the slopes and rainfall intensities in Table 1 were classified as follows:

Low intensity: $r < 40 \text{ mm h}^{-1}$; mild slope: $S < 10\%$

High intensity: $40 < r < 80 \text{ mm h}^{-1}$; steep slope: $10 < S < 20 \%$

Very high intensity: $r > 80 \text{ mm h}^{-1}$; very steep slope: $S > 20\%$

Table 2 summarizes the results in Table 1 by considering the above classifications on slope and rainfall intensity. Table 2 presents which model performed better depending upon slope and rainfall intensity conditions. According to Table 2, the velocity approach (V) performed better over mild and steep slopes, under low rainfall intensity. The USP model performed better over mild and steep slopes, under high rainfall intensity and over mild slopes, under very high rainfall intensity. The SS and SP models performed better over very steep slopes, under high rainfall intensity. The ANN model performed better than the physically-based models in estimating observed mean sediment discharge loads from steep, and very steep slopes, under very high rainfall intensity. It also performed better over very steep slopes, under low rainfall intensity.

Table 2 Performance of models, showing best performance depending upon slope and rainfall intensity.

	Mild slope	Steep slope	Very steep slope
Low intensity	V	V	ANN
High intensity	USP	USP	SS, SP
Very high intensity	USP	ANN	ANN

CONCLUDING REMARKS

In this study, the modelling of nonsteady-state sheet sediment transport by ANNs was accomplished. The application of the model to simulate sediment loads from different slopes under different rainfall intensities indicated that the ANNs model could perform as well as, in some cases better than, the physically-based models.

The performance of the ANNs and physically-based models, depending upon rainfall intensity and slope steepness, is summarized in Table 2. When modelling sediment loads from bare surfaces, hydrologists could take the results in Table 2 into consideration when deciding on which model to employ.

Generally, the physically-based sheet sediment transport models involve numerical solutions of nonlinear partial differential equations. On the other hand, numerical schemes generally require iterative methods for the solutions of nonlinear difference equations and they are prone to convergence and instability problems. In addition to the numerical problems, the physically-based models of sheet sediment transport require the values of many model parameters at the model grid scale for realistic simulations. In practice, however, such data are rarely available. When one considers the numerical and data availability problems related to the physically-based models,

the much simpler ANN model could be a very practical and promising modelling tool for hydrologists to study sediment transport processes.

REFERENCES

- ASCE Task Committee on Application of Artificial Neural Networks in Hydrology (2000a) Artificial neural networks in hydrology, I: preliminary concepts. *J. Hydrol. Engng ASCE* **5**(2), 115–123.
- ASCE Task Committee on Application of Artificial Neural Networks in Hydrology (2000b) Artificial neural networks in hydrology, II: hydrologic applications. *J. Hydrol. Engng ASCE* **5**(2), 124–137.
- Alonso, C. V., Neibling, W. H. & Foster, G. R. (1981) Estimating sediment transport capacity in watershed modeling. *Trans. Am. Soc. Agric. Engrs* **24**, 1211–1220.
- Aziz, A. R. A. & Wong, K. F. V. (1992) Neural network approach to the determination of aquifer parameters. *Ground Water* **30**(2), 164–166.
- Cannon, A. J. & Whitfield, P. H. (2002) Downscaling recent streamflow conditions in British Columbia, Canada using ensemble neural network models. *J. Hydrol.* **259**, 136–151.
- Dawson, W. C. & Wilby, R. (1998) An artificial neural network approach to rainfall–runoff modeling. *Hydrol. Sci. J.* **43**(1), 47–66.
- Elshorbagy, A., Panu, U. S. & Simonovic, S. P. (2001) Analysis of cross-correlated chaotic streamflows. *Hydrol. Sci. J.* **46**(5), 781–794.
- Foster, G. R. (1982) Modeling the erosion process. In: *Hydrologic Modeling of Small Watersheds* (ed. by C. T. Haan, H. P. Johnson & D. L. Brakensiek), 295–380. Am. Soc. Civil Engrs, New York, USA.
- Govindaraju, R. S. & Kavvas, M. L. (1991) Modeling the erosion process over steep slopes: approximate analytical solutions. *J. Hydrol.* **127**, 279–305.
- Guldal, V. & Muftuoglu, R. F. (2001) 2D unit sediment graph theory. *J. Hydrol. Engng ASCE* **6**(2), 132–140.
- Halfi, A. H., Halfi, H. M. & Azmoodeh, M. (1993) Predicting runoff from rainfall using artificial neural networks. *Proc. Engng. Hydrol. ASCE* 760–765.
- Hsu, K., Gupta, H. V., Soroshian, S. & Gao, X. (1996) An artificial neural network for rainfall estimation from satellite infrared imaginary. In: *Applications of Remote Sensing in Hydrology* (Proc. Third Int. Workshop), NHRI Symp. no.17, NASA, Greenbelt, Maryland, USA.
- Huang, W. & Foo, S. (2002) Neural network modeling of salinity in Apalachicola River. *Wat. Research* **36**(1), 356–362.
- Kang, K. W., Kim, J. H., Park, J. C. & Ham, K. J. (1993) Evaluation of hydrological forecasting system based on neural network model. In: *Proc. 25th Congress of IAHR*, 257–264. IAHR, Delft, The Netherlands.
- Kilinc, M. & Richardson, E. V. (1973) Mechanics of soil erosion from overland flow generated by simulated rainfall. Paper 63, Hydrology Papers, Colorado State University, Fort Collins, Colorado, USA.
- Leaf, C. (1974) A model for predicting erosion and sediment yield from secondary forest road construction. Forest Service Research note RM–274, Rocky Mountain Forest and Range Exper. Station, US Dept. Agric., Fort Collins, Colorado, USA.
- Li, R. M. (1979) Water and sediment routing from watersheds. In: *Modeling of Rivers* (ed. by H. W. Shen), 9.1–9.88. John Wiley & Sons Inc., New York, USA.
- Maier, H. R. & Dandy, G. C. (1996) The use of artificial neural networks for the prediction of water quality parameters. *Wat. Resour. Res.* **32**(4), 1013–1022.
- Marcus, M., Salas, J. D. & Shin, H.-K. (1995) Predicting streamflows based on neural networks. In: *Proc. First Int. Conf. on Water Resources Engineering*, 1641–1646. Am. Soc. Civil Engrs, New York, USA.
- Megahan, W. F. (1974) Erosion over time on several distributed granitic soils: a model. Forest Service Research Paper INT–156, Intermountain Forest and Range Exper. Station, US Dept. Agric., Ogden, Utah, USA.
- Moore, I. D. & Burch, G. J. (1986) Sediment transport capacity of sheet and rill flow: application of unit stream power theory. *Wat. Resour. Res.* **22**(8), 1350–1360.
- Morshed, J. & Kaluarachchi, J. J. (1998) Parameter estimation using artificial neural network and genetic algorithm for free-product and recovery. *Wat. Resour. Res.* **34**(5), 1101–1113.
- Persson, M., Berndtsson, R. & Sivakumar, B. (2001) Using neural networks for calibration of time-domain reflectometry measurements. *Hydrol. Sci. J.* **46**(3), 389–398.
- Rose, C. W., Williams, J. R., Sander, G. C. & Barry, D. A. (1983a) A mathematical model of solid erosion and deposition processes. I. Theory for a plane land element. *Soil Sci. Soc. Am. J.* **47**(5), 991–995.
- Rose, C. W., Williams, J. R., Sander, G. C. & Barry, D. A. (1983b) A mathematical model of solid erosion and deposition processes. II. Application to data from an arid zone catchment. *Soil Sci. Soc. Am. J.* **47**(5), 996–1000.
- Sharma, P. P., Gupta, S. C. & Foster, G. R. (1993) Predicting soil detachment by raindrops. *Soil Sci. Soc. Am. J.* **57**, 674–680.
- Smith, R. E. (1976) Simulation erosion dynamics with a deterministic distributed watershed model. In: *Proc. Third Federal Interagency Sedimentation Conference*, vol. 1, 163–173. Water Resources Council, Washington, DC, USA.
- Smith, J. & Eli, R. N. (1995) Neural-network models of rainfall–runoff process. *J. Wat. Resour. Plan. Manage. ASCE*, **121**(6), 499–508.
- Tawfik, M., Ibrahim, A. & Fahmy, H. (1997) Hysteresis sensitive neural network for modeling rating curves. *J. Comput. Civil Engng ASCE* **11**(3), 206–211.
- Tayfur, G. (2001) Modeling two dimensional erosion process over infiltrating surfaces. *J. Hydrol. Engng ASCE* **6**(3), 259–262.

- Tayfur, G. (2002) Applicability of sediment transport capacity models for non-steady state erosion from steep slopes. *J. Hydrol. Engng ASCE* 7(3), 252–259.
- Tayfur, G., Kavvas, M. L., Govindaraju, G. S. & Storm, D. E. (1993) Applicability of St Venant equations for two-dimensional overland flows over rough infiltrating surfaces. *J. Hydraul. Engng ASCE* 119(1), 51–63.
- Tohma, S. & Igata, S. (1994) Rainfall estimation from GMS imagery data using neural networks. *Hydraul. Engng Software V*, vol. 1 (ed. by W. R. Blain & K. L. Katsifarakis), 121–130. Computational Mechanics, Southampton, UK.
- Tokar, A. S. & Johnson, P. A. (1999) Rainfall–runoff modeling using artificial neural networks. *J. Hydrol. Engng ASCE*, 4(3), 232–239.
- Woolhiser, D. A. (1974) Unsteady free-surface flow problems. In: *Proc. Int. Symp. on Unsteady Flow in Open Channels*, 195–213. Colorado State University, Fort Collins, Colorado, USA.
- Woolhiser, D. A., Smith, R. E. & Goodrich, D. C. (1990) *KINEROS: A Kinematic Runoff and Erosion Model: Documentation and User Manual*. Report ASR-77, US Dept of Agriculture, Agriculture Research Service.
- Yang, C. T. (1996) *Sediment Transport Theory and Practice*. McGraw-Hill, New York, USA.

Received 4 September 2001; accepted 5 July 2002